CrystEngComm

Accepted Manuscript

ROYAL SOCIETY OF CHEMISTRY

www.rsc.org/crystengcomm

Journal Name

RSCPublishing

ARTICLE

Metal-Organic Frameworks with Improved Moisture Stability Based on a Phosphonate Monoester: Effect of Auxiliary N-donor Ligands for Framework Dimensionality

Cite this: DOI: 10.1039/xoxxoooooox

Received ooth January 2012,
Accepted ooth January 2012

DOI: 10.1039/xoxxoooooox

www.rsc.org/

Jian-Wei Zhang,[ab] Cui-Cui Zhao,[a] Yin-Ping Zhao,[a] Hai-Qun Xu,[b] Zi-Yi Du*[ac] and Hai-Long Jiang*[bc]

A series of metal-organic frameworks (MOFs) with structures from 1D chain, 2D layer or double layer to 3D network have been successfully obtained based on phosphonate monoester ligand in the presence of auxiliary N-donor ligands. The phosphonate monoester behaving as a carboxylate linker bridges to metal ions while the auxiliary N-donor ligands play a crucial role in both structural diversity and dimensionality variation of the resultant MOFs. Remarkably, the hydrophobic ethyl groups involved in the phosphonate monoester linker offer protection/shield for hydrolytically vulnerable M-O bonds, resulting in the MOFs highly moisture stable as expected. The porous MOFs with 3D network have shown CO_2 adsorption and strong fluorescence emissions.

Introduction

During the last two decades, as a relatively new type of porous crystalline materials, metal-organic frameworks (MOFs), also called porous coordination polymers, have attracted widespread attention due to their modular assembly, structural diversity, chemical tailorability and tunability, as well as potential applications in many fields, such as, gas sorption and separation, catalysis, sensing, drug delivery, and so on.[1-5] In comparison of traditional porous materials, such as, zeolites, activated carbon and mesoporous silica, it is fair to say that MOFs have many advantages, especially for their crystallinity, tunability and modular nature, which allow MOF pore sizes ranging from ultramicroporous to mesoporous (0-4 nm or even larger). Thus it is considered that MOFs with wide pore size range bridge the gap between mesoporous silica with large pores and zeolites with very small pores.[3c] However, most of the previously reported MOFs are moisture sensitive, which has being recognized as an imperative issue on the way to their practical applications. For example, as a classical and representative MOF, MOF-5 has been intensively studied for different ends, while the involved Zn_4O clusters are readily hydrolyzed upon exposure to water vapor, giving rise to porous structure collapse or/and phase change.[6] So far, there are mainly several types of stable MOFs reported, zeolitic imidazolate frameworks (ZIFs) and MIL-series, UiO-series, pyrazolates and triazolates, etc.,[7-8] which have been intensively studied for functional applications. Considering that the moisture sensitivity of MOFs could be caused by the weak metal-carboxylic oxygen bonds that are readily attacked by water molecules, we and others have recently developed a series of MOFs with very high chemical stability based on the combination between "hard acid" zirconium(IV) and "hard base" carboxylate anions.[9,10]

To continue such research line on targeting MOFs with enhanced moisture stability, we are interested in the MOFs linked by organic phosphonate monoesters. Although phosphonic acid has been widely employed as organic linkers for the synthesis of metal phosphonates,[11] organic phosphonate monoesters are underexplored class of ligands.[12] Recently, the bidentate oxygen donor ligation in phosphonate monoesters has been reported to behavior as carboxylate-like coordination mode.[12c-e] The phosphonate monoester allows its self-assembly process with metal ions proceed moderately to yield single crystals with suitable sizes. Moreover, it has been reported that moisture resistance of MOF can be obtained by postsynthetically grafting alkyl group onto organic linkers.[13] Therefore, the hydrophobic alkyl group (-R) tethered on the ligand might functionalize a sterically shield to protect the hydrolytically vulnerable M-O bonds and thus enhance the moisture stability of the resultant MOFs. Bearing these in mind, 4,4'-biphenyldiphosphonate bis(monoethyl ester) (H_2BPDP), has been isolated first, followed by assembly with auxiliary N-donor ligand, bis(imidazol-1-yl)methane (BIM) or 1,3,5-tri(1H-imidazol-1-yl)benzene (TIB) to afford a series of MOFs from 1D chain, [Cd(BPDP)(BIM)(H_2O)$_2$] (**1**), to double layered [Cd(BPDP)(BIM)]•7H_2O (**2**) and layered [Co(BPDP)(TIB)(H_2O)]•7H_2O (**3**), to 3D isomorphous frameworks, [M(BPDP)(TIB)(H_2O)$_2$]•6H_2O (M = Cd for **4**, Co for **5**, and Cu for **6**). It is very interesting that the coordination between BPDP ligand and metal ions only gives 1D chain in all MOFs, while the introduction of an auxiliary N-donor ligand

extends the 1D chain to different framework dimensionalities. Remarkably, these MOFs based on phosphonate monoester linker with ethyl group protection are highly moisture stable as expected, and compounds **4** and **6** have shown the capability for CO_2 adsorption, revealing the permanent porosity upon solvent removal. The Cd-based MOFs have also shown strong fluorescence emissions assigned to intraligand transitions.

Experimental section

Materials and general methods

All solvents and reagents for syntheses were commercially available and used as received, except for that organic ligands were synthesized using published procedures with modifications (See Electronic Supplementary Information, ESI).[14] The FT-IR spectra were recorded on a Perkin-Elmer Spectrum 2000 FT-IR spectrometer using KBr pellets in the range of 4000-400 cm^{-1}. Thermogravimetric analyses (TGA) were carried out on a Shimadzu DTG-60H thermogravimetric-differential thermal analyzer at a ramp rate of 10 °C/min in nitrogen. Powder X-ray diffraction patterns (XRD) were obtained on a Japan Rigaku SmartLab^{TM} rotation anode X-ray diffractometer equipped or Holland X'Pert PRO fixed anode X-ray diffractometer equipped with graphite monochromatized Cu Kα radiation (λ = 1.54178 Å). Solid state emission spectra were investigated on a Perkin-Elmer LS55 luminescence spectrophotometer under the same measurement conditions. The CO_2 adsorption/desorption isotherms were conducted using a Micrometritics ASAP 2020 system and the sorption temperatures were controlled by dry ice/acetone bath. Compound **4** was dried under a dynamic vacuum at 120 °C for 24 h. Before the measurement, the sample was dried again by using the "outgas" function of the surface area analyzer for 6 h at 120 °C. Compound **6** was subjected to solvent exchange (by soaking in methanol for over 1 day) and then treated by the same process as compound **4** prior to the adsorption/desorption measurement.

Preparations of compounds 1-6

Preparation of [Cd(BPDP)(BIM)(H_2O)$_2$] (1)

A mixture of H_2BPDP (74 mg, 0.2 mmol) with BIM (30 mg, 0.2 mmol) in 4 mL distilled water was introduced drop by drop into $Cd(CH_3COO)_2$•$2H_2O$ (53 mg, 0.2 mmol) in 4 mL distilled water under vigorous stirring. The resultant solution was filtered to give a filtrate. The filtrate was allowed to be heated and spontaneously volatilized at ~80 ^oC for about 2 hours in a beaker to afford colorless plate-shaped single crystals of compound **1**. The measured XRD pattern is in good agreement with the one simulated from crystal structure data. IR data (KBr, cm^{-1}): 3124 (m), 2974 (m), 1500 (m), 1400 (m), 1283 (m), 1238 (m), 1197 (s), 1143 (m), 1041 (s), 936 (m), 828 (m), 766 (m), 650 (m), 593 (m), 544 (m), 482(m).

Preparation of [Cd(BPDP)(BIM)]•7H_2O (2)

A mixture of $Cd(NO_3)_2$•$4H_2O$ (31 mg, 0.1 mmol) with BIM (15 mg, 0.1 mmol) in 2 mL ethanol was introduced drop by drop into a 4 mL hot ethanol solution of H_2BPDP (55 mg, 0.15 mmol), which allows vigorous stirring under heated condition followed by filtration. The filtrate was heated at 65 ^oC in 20 mL vial for 1 day to yield colorless rod-shaped crystals of **2**. The pure phase of compound **2** has not been obtained although much effort was exerted.

Preparation of [Co(BPDP)(TIB)(H_2O)]•7H_2O (3)

A mixture of $Co(CH_3COO)_2$•$4H_2O$ (25 mg, 0.1 mmol) with TIB (28 mg, 0.1 mmol) in 1 mL ethanol and 1 mL distilled water was introduced drop by drop into a 4 mL hot ethanol solution of H_2BPDP (55 mg, 0.15 mmol), which allows vigorous stirring under heated condition followed by filtration. The filtrate was heated at 65 ^oC in 20 mL vial for 1 day to yield pink plate-shaped crystals of **3**. The measured XRD pattern is in good agreement with the one simulated from crystal structure data. IR data (KBr, cm^{-1}): 3252 (m), 3113 (m), 1619 (m), 1561 (m), 1506 (vs), 1389 (m), 1309 (w), 1278 (m), 1143 (w), 1076 (m), 1014 (m), 931 (w), 874 (m), 812 (w), 757 (m), 676(w), 638 (m).

Preparation of [M(BPDP)(TIB)(H_2O)$_2$]•6H_2O (M = Cd for 4, and Co for 5)

The two compounds were prepared in a similar procedure to that of **3** except that $Co(CH_3COO)_2$•$4H_2O$ was replaced by $Cd(NO_3)_2$•$4H_2O$ for **4** and $Co(NO_3)_2$•$6H_2O$ for **5**. Colorless and pink block-shaped crystals of **4** and **5** were obtained, respectively.The measured XRD pattern of compound **4** is in good agreement with the one simulated from crystal structure data while the pure phase of compound **5** has not been obtained. IR data for **4** (KBr, cm^{-1}): 3376 (m), 3129 (m), 1622 (m), 1513 (m), 1381 (s), 1343 (m), 1177 (s), 1045 (vs), 937 (m), 826 (m), 759 (s), 646 (w), 586 (m), 525 (s), 462 (m).

Preparation of [Cu(BPDP)(TIB)(H_2O)$_2$]•6H_2O (6)

A 4 mL aqueous solution (~75 ^oC) of $Cu(NO_3)_2$•$3H_2O$ (93 mg, 0.2 mmol) was added dropwise into a mixture of H_2BPDP (93 mg, 0.25 mmol) with TIB (55 mg, 0.2 mmol) in 4 mL distilled water (~75 ^oC). The resultant solution was filtered to give a filtrate, which was allowed to be heated and spontaneously volatilized at ~75 ^oC for about 2 hours in a beaker to yield green block-shaped crystals of **6**. The measured XRD pattern is in good agreement with the one simulated from crystal structure data. IR data (KBr, cm^{-1}): 3122 (m), 2974 (w), 1618 (m), 1507 (s), 1292(m), 1248 (m), 1179 (s), 1136 (w), 1046(vs), 934 (s), 827(m), 757 (m), 594 (m), 518 (m).

X-ray crystallography

Single crystal X-ray data collection for the organic ligands and all coordination compounds were performed on a Smart ApexII CCD diffractometer equipped with a graphite-monochromated Mo-*K*α radiation (*λ* = 0.71073 Å). Intensity data for all compounds were collected at 296 K. The data sets were corrected for Lorentz and polarization factors as well as for absorption by SADABS program.[15] All structures were solved by the direct method and refined by full-matrix least-squares fitting on *F*2 by SHELX-97.[16] C-bound H atoms were generated geometrically while O-bound H atoms were located in the difference Fourier map. All non-hydrogen atoms were refined with anisotropic thermal parameters whereas all hydrogen atoms were refined isotropically. The hydrogen atoms for the water molecules in compounds **3-6** are not included in the refinements. The contribution of the disordered water

molecules removed by the SQUEEZE process[17] for compounds **2**, **4**, **5** and **6** has been included in Table 1. The number of isolated water molecules for compounds **2**, **4**, **5** and **6** can be

Complexes	Phosphonate monoester	Phosphonate diester	**1**	**2**
Formula	$C_{18}H_{24}O_6P_2$	$C_{22}H_{32}O_6P_2$	$C_{25}H_{34}N_4O_8P_2Cd$	$C_{32}H_{52}O_{13}N_8P_2Cd$
Fw	398.31	454.42	692.90	931.16
Space group	*P*-1	$P2_1/c$	*P*-1	*C*2/*m*
a (Å)	7.6515(2)	15.8384(8)	8.9485(4)	17.4704(16)
b (Å)	8.0147(2)	8.4589(5)	13.0362(6)	28.935(2)
c (Å)	9.3307(2)	17.7369(11)	13.0950(6)	8.6998(7)
α (deg)	71.162(2)	90	82.8370(10)	90
β (deg)	67.620(2)	96.493(2)	71.0060(10)	113.244(2)
γ (deg)	84.036(2)	90	87.4860(10)	90
V (Å^3)	500.64(2)	2361.1(2)	1433.14(11)	4040.8(6)
Z	1	4	2	4
$d_{calcd.}$ (g/cm^3)	1.321	1.278	1.606	1.531
μ(mm^{-1})	0.247	0.218	0.928	0.691
F(000)	210	968	708	1928
Reflections collected	4320	11617	11557	16813
Independent reflections	2254	4634	5563	4064
Obsd data [I>2σ(I)]	1431	2339	4817	2728
Data/restraints/parameters	2254 / 0 / 118	4634 / 0 / 271	5563 / 9 / 376	4064 / 2 / 225
GOF on F^2	1.042	1.000	1.035	1.008
$R1$,[a] $wR2$[b] [I > 2σ(I)]	0.0518, 0.1208	0.0578, 0.1142	0.0272, 0.0709	0.0533, 0.1245
$R1$,[a] $wR2$[b] (all data)	0.0854, 0.1383	0.1295, 0.1422	0.0326, 0.0747	0.0813, 0.1369

Table 1. Crystallographic parameters for ligands and compounds **1–6** from single crystal X-ray diffraction.

Complexes	**3**	**4**	**5**	**6**
Formula	$C_{33}H_{50}O_{14}N_6P_2Co$	$C_{33}H_{50}CdN_6O_{14}P_2$	$C_{33}H_{50}CoN_6O_{14}P_2$	$C_{33}H_{50}CuN_6O_{14}P_2$
Fw	875.67	929.13	875.66	880.27
Space group	$P2_1/c$	*C*2/*c*	*C*2/*c*	*C*2/*c*
a (Å)	10.2738(2)	21.7570(3)	21.5310(4)	21.6074(6)
b (Å)	20.8895(5)	14.2474(2)	14.1050(2)	14.0197(4)
c (Å)	19.9247(5)	14.6058(2)	14.5410(2)	14.4710(4)
α (deg)	90	90	90	90
β (deg)	97.822(2)	118.1600(10)	117.4320(10)	117.832(2)
γ (deg)	90	90	90	90
V (Å^3)	4236.34(17)	3991.61(10)	3919.48(11)	3876.58(19)
Z	4	4	4	4
$d_{calcd.}$ (g/cm^3)	1.373	1.546	1.484	1.508
μ(mm^{-1})	0.549	0.700	0.593	0.721
F(000)	1836	1920	1836	1844
Reflections collected	29020	16614	16275	14321
Independent Reflections	8332	3918	3847	3807
Obsd data [I>2σ(I)]	4923	3047	2725	2005
Data/restraints/parameters	8332 / 3 / 505	3918 / 1 / 229	3847 / 1 / 229	3807 / 1 / 229
GOF on F^2	1.019	1.049	1.062	0.995
$R1$,[a] $wR2$[b] [I > 2σ(I)]	0.0670, 0.1660	0.0376, 0.1003	0.0532, 0.1408	0.0640, 0.1284
$R1$,[a] $wR2$[b] (all data)	0.1234, 0.1972	0.0497, 0.1051	0.0738, 0.1500	0.1212, 0.1452

[a] $R_1 = \Sigma||F_o| - |F_c||/\Sigma|F_o|$. [b] $wR_2 = \{\Sigma[w(F_o^2 - F_c^2)^2]/\Sigma w(F_o^2)^2]\}^{1/2}$.

Table 2. Selected bond lengths (Å) for compounds **1-6**

		1	
Cd(1)–O(1)	2.323(2)	Cd(1)–N(1)	2.324(2)
Cd(1)–O(1W)	2.368(2)	Cd(2)–O(5)	2.261(2)
Cd(2)–N(2)	2.262(2)	Cd(2)–O(2W)	2.414(2)
		2	
Cd(1)–N(1)	2.306(4)	Cd(1)–O(1)	2.313(3)
Cd(1)–N(3)	2.320(4)		
		3	
Co(1)–O(2)	2.065(3)	Co(1)–O(4)#1	2.079(3)
Co(1)–N(4)#2	2.110(4)	Co(1)–N(6)#3	2.115(4)
Co(1)–N(2)	2.130(4)	Co(1)–O(1W)	2.215(3)
		4	
Cd(1)–N(2)#1	2.248(2)	Cd(1)–N(2)	2.248(2)
Cd(1)–O(1W)	2.354(2)	Cd(1)–O(1)	2.362(2)
		5	
Co(1)–N(2)#1	2.105(3)	Co(1)–N(2)	2.105(3)
Co(1)–O(1W)	2.138(2)	Co(1)–O(1)	2.177(2)
		6	
Cu(1)–N(2)#1	1.999(3)	Cu(1)–N(2)	1.999(3)
Cu(1)–O(1W)	2.050(3)	Cu(1)–O(1)	2.402(3)

Symmetry codes: #1, –x, y – 1/2, –z + 3/2; #2, –x + 1, y + 1/2, –z + 3/2; #3, x – 1, y, z.

estimated by the contribution of the electrons removed from the unit-cell contents, and the detailed information can be found in the CIF files (see _platon_squeeze_details). For the structures of compounds **4-6**, the position disorder of C(18) and N(4) atoms in one non-coordinated imidazole group of the TIB ligand is refined anisotropically using the PART, EXYZ and EADP instructions of SHELXL. Crystallographic data and structural refinements are summarized in Table 1. Important bond lengths are listed in Table 2.

Results and discussion

Monoester and diester ligands

In each phosphonate group, there are three O atoms connected to P atom; one O atom binds to P center with double bonds while the other two O atoms bind to P center with single bond in hydroxide or esterification form. If both oxygen atoms are esterified (ESI, Fig. S1), the phosphonate diester group would be difficult to coordinate to any metal cations. If one oxygen atom is esterified (ESI, Fig. S2), the phosphonate monoester group might behave as carboxylic acid group to coordinate to metal cations and afford MOFs. Therefore, the monoester was employed for the following MOF synthesis.

Cd(BPDP)(BIM)$(H_2O)_2$ (1)

Compound **1** crystallizes in the *P*-1 space group. It contains two crystallographically unique cadmium(II) ions, two independent bridging ligands (BPDP and BIM) and two aqua ligands in the asymmetric unit. The unique Cd(1) and Cd(2) cations locate at two independent inversion centers, respectively, and each is octahedrally coordinated by three pairs of symmetry-related donors, *i.e.*, two O atoms from two phosphinate ligands, two N atoms from two BIM ligands, and two aqua ligands (Fig. 1). The water-bound O-Cd lengths (2.368(2) and 2.414(2) Å) are slightly longer than those of the PO_3-bound ones (2.261(2) to 2.323(2) Å), all of which are comparable to reported cadmium(II) MOFs.[4b,18]

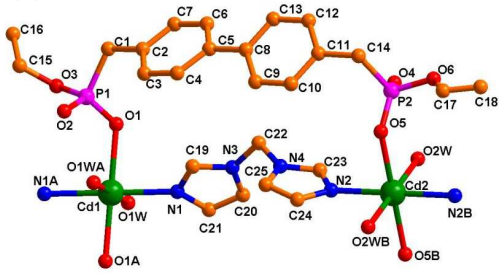

Fig. 1 Coordination environment of cadmium(II) centers and the binding fashion of BPDP and BIM ligands in compound **1**. Symmetry codes: A. -x, 2-y, 1-z; B. 2-x, 1-y, 1-z.

The BPDP and BIM ligands both act as a bidentate bridging ligand in an end-to-end fashion (Fig. S3), and the interconnection of the Cd(II) ions by the above two types of ligands forms a 1D double-chain (Fig. 2a), which features an asymmetric four-member ring unit containing one BPDP, one BIM and two Cd(II) ions. The corner-sharing of such ring units at the Cd(II) inversion centers constitutes the unique double-chain running along the *b*-axis. The discrete double-chains in compound **1** are further assembled into a compact three-dimensional structure via van der Waals forces and there exists no lattice water molecules in the whole structure (Fig. 2b).

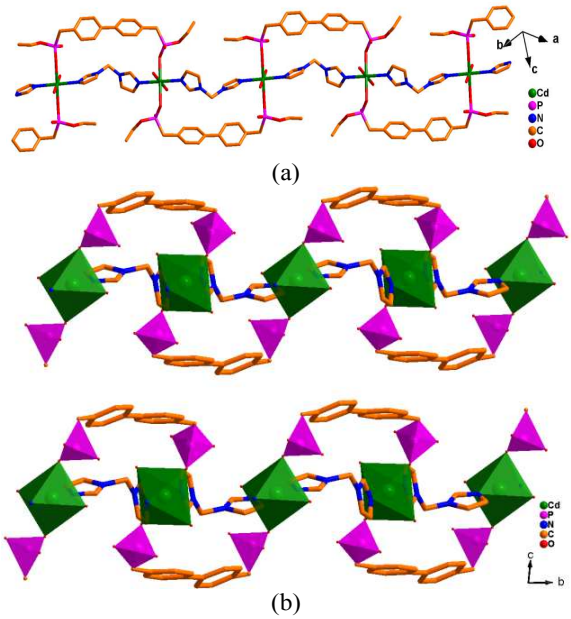

Fig. 2 (a) View of the 1D double-chain structure of **1**. (b) View of the overall structure of **1** down the *a*-axis. The CdO_2N_4 and PCO_3 polyhedra are shaded in olive and pink, respectively.

[Cd(BPDP)(BIM)]•7H_2O (2)

When the cadmium(II) source $Cd(CH_3COO)_2$•$2H_2O$ in the synthesis of compound **1** was replaced by $Cd(NO_3)_2$•$4H_2O$ in ethanol, compound **2** was obtained with a double layered structure crystallizing in the *C*2/*m* space group. There are one crystallographically independent cadmium(II) ion lying on a 2-fold axis, one unique BPDP ligand related by 2-fold symmetry, and two types of BIM ligands related by 2-fold and mirror symmetries, respectively, in the asymmetric unit. The Cd(II) ion is coordinated in a pseudo-octahedron environment by four nitrogens from four BIM ligands and two oxygens from two BPDP ligands (Fig. 3). The Cd-O and Cd-N bond distances are in a narrow and normal range of 2.306(4)-2.320(4) Å. Similar to that in compound **1**, the BPDP ligand is bidentate and bridges to two Cd(II) with two oxygens from P-O single bonds to form a 1D chain. In comparison, each of the two unique BIM ligands bridge two Cd(II) with two nitrogens to give a nanoribbon-like chain along the *a*-axis with ribbon width of 1.67 nm in the *b*-direction (ESI, Fig. S4). The two kinds of chains are interconnected from different directions to construct a 2D thick double layer in the *ac* plane, in which the quadrangle-like rings are composed by four Cd(II), two BPDP and two BIM ligands (Fig. 4). The thickness of the double layer is about 16.7 Å and the inter-double-layer distance is 14.5 Å. In this case, the different double layers almost stack together without interlayer openings (ESI, Fig. S4c).

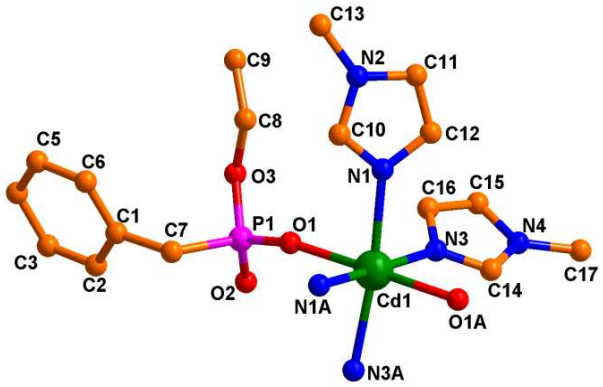

Fig. 3 Coordination environment of cadmium(II) center and the binding fashion of BPDP and BIM ligands in compound **2**. Symmetry code: A 1-x, y, 2-z.

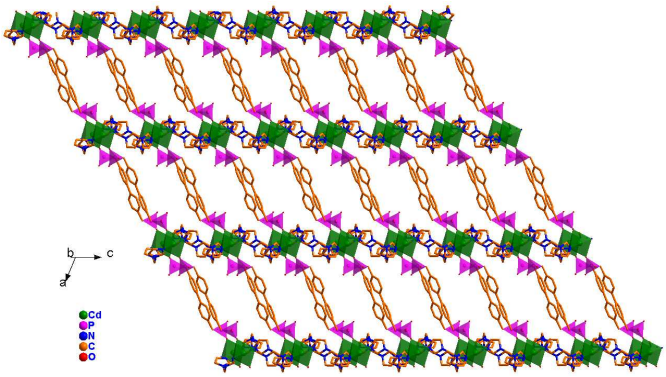

Fig. 4 View of the 2D thick double layer in the structure of compound **2** along the *b*-axis. The CdO_2N_4 and PCO_3 polyhedra are shaded in olive and pink, respectively.

[Co(BPDP)(TIB)(H_2O)]•7H_2O (3)

By replacing Cd(II) with Co(II) and BIM with TIB, compound **3** in $P2_1/c$ space group with similar 2D sheet was successfully obtained. As shown in Fig 5, the asymmetric unit of **3** consists of one Co(II) center, one BPDP, one TIB and one aqua ligand as well as seven lattice water molecules. The Co(II) ion is six coordinated by three nitrogens from three TIB ligands and two oxygens from two BPDP ligands as well as an aqua ligand. Like that in compound **1**, the water O-Co bond distance of 2.215(3) Å is slightly longer than those of the O-Co bonds of phosphonate ligand and N-Co bonds of TIB ligand, ranging from 2.065(3) to 2.128(4) Å, which are comparable to reported cobalt(II) MOFs.[19] Each of the two oxygens with P-O single bond in BPDP ligand connects one Co(II) to form a 1D wave-like chain and the depth of "wave" is a little bit less than that in compound **1**. Each nitrogen of TIB ligand bridges to one Co(II) cation to provide a 2D graphene-like layer in *ab* plane with large 6-member rings, which is formed by three Co(II) and three TIB ligands (ESI, Fig. S5). As a result, the Co-BPDP chains are grafted onto the Co-TIB layer to by N-Co-O connectors to eliminate the large rings and result in a layer not only a little bit thicker but also more "solid" (Fig. 6; ESI, Fig. S5c). The interlayer distance is about 10 Å in the *c*-axis direction. From the topological perspective, the BPDP ligand can be viewed as a metal linker, while the Co(II) center and TIB ligand can be defined as 5- and 3-connected nodes, respectively, and the interconnection of the two kinds of nodes

in a 1:1 ratio gives a two-dmensional (3,5)-connected net (Fig 6b).

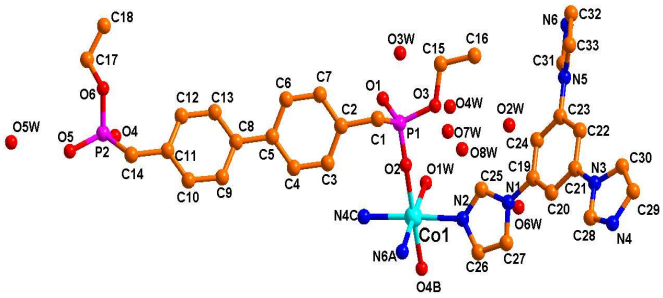

Fig. 5 Coordination environment of cadmium(II) center and the binding fashion of BPDP and TIB ligands in compound **3**. Symmetry code: A -1+x, y, z; B -x, -0.5+y, 1.5-z; C 1-x, 0.5+y, 1.5-z .

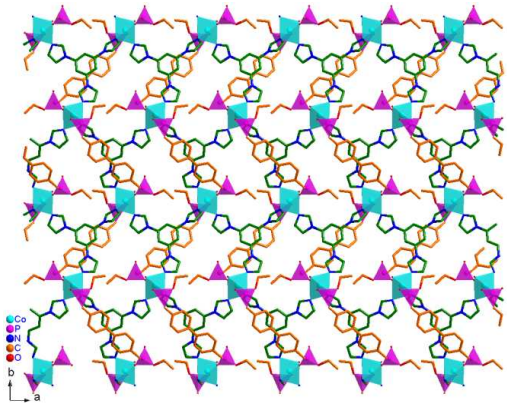

(a)

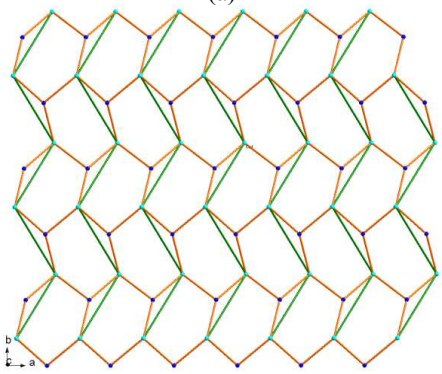

(b)

Fig. 6 (a) View of the 2D layered structure of compound **3** along the *c*-axis. The CoO_2N_4 and PCO_3 polyhedra are shaded in cyan and pink, respectively. The C atoms in TIB ligand are drawn in olive for its clear recognition. (b) Topological view of the (3,5)-connected 2D layer, in which the TIB ligand and Cd(II) are simplified as 3- and 5-connected nodes (blue and cyan atoms), respectively, and the BPDP ligand is simplified as a line in olive.

[M(BPDP)(TIB)$(H_2O)_2$]•7H_2O (M = Cd 4, Co 5, Cu, 6)

It is very interesting that metal nitrate as metal source in aqua media seems to be ben
eficial to MOFs with 3D frameworks in our system. By replacing $Co(CH_3COO)_2$•4H_2O with $Cd(NO_3)_2$•4H_2O or $Co(NO_3)_2$•6H_2O only while fixing other reaction parameters as those for compound **3**, compounds **4** and **5** with 3D networks were obtained. Similarly, by employing $Cu(NO_3)_2$•3H_2O as metal source and slightly changing reaction conditions, 3D structured compound **6** was prepared. The unit-cell dimensions, volumes, related bond distances, and angles of compounds **4-6** are only slightly different. They are isomorphous and exhibit similar structures. Therefore, compound **4** will be discussed in detail as a representative. As shown in Fig 7, there is one crystallographically unique Cd(II) ion with half-occupancy locating at an inversion center, a half BPDP locating at another inversion center and a half TIB ligand lying about a two-fold axis as well as one aqua ligand in its asymmetric unit. Almost the same as that in compound **1**, the Cd(II) is pseudo-octahedrally coordinated by two nitrogens from two TIB ligands and four oxygen atoms, in which two oxygens are from two BPDP ligands and the other two oxygens come from aqua ligands. The phosphonate and aqua O-Cd bond distances are similarly 2.363(2) and 2.352(3) Å, respectively; the Cd-N bond distance is 2.246(3) Å, all of which falls in normal ranges.[18] As previously, the BPDP ligand also acts a bridge to connect two Cd(II) to give a wave-like chain. Strikingly, the TIB ligand is not commonly three coordinated but only bridges to two Cd(II) with its two nitrogens, while the third nitrogen atom remains uncoordinated and exhibits substitutional disorder with the neighbouring C18 atom. Such connection makes Cd-TIB also a wave-like chain with deeper "wave" than that for Cd-BPDP (ESI, Fig. S6). The cross interconnection of these two kinds of wave-like chains leads to a 3D framework with 1D nanochannels of 9.7 × 13.0 $Å^2$ along the *b*-axis (Fig. 8a). The ester groups of BPDP ligand are toward the channels. The effective free volume is about 18.2% calculated by PLATON.[20] As described above, the Cd(II) ion can be regarded as a four-connected node while both BPDP and TIB ligands can be simplified as lines, thus the whole network can be extended to a 4-connected $CdSO_4$ net with the Schläfli symbol (6^5•8) (Fig. 8b).[21]

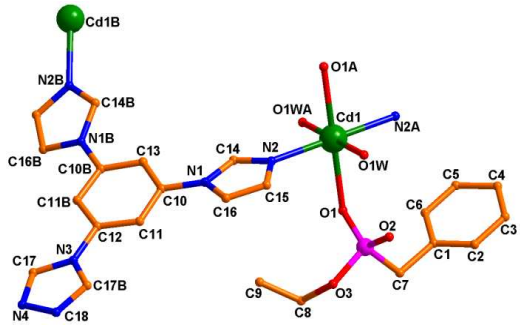

Fig. 7 Coordination environment of cadmium(II) center and the binding fashion of BPDP and TIB ligands in compound **4**. Symmetry code: A 0.5-x,0.5-y,1-z; B 1-x, y, 1.5-z. The atoms marked as N4 and C18 indicate their substitutional disorder.

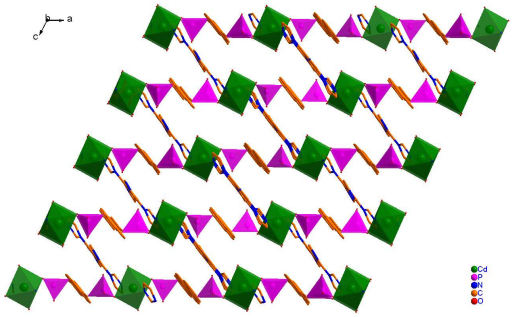

(a)

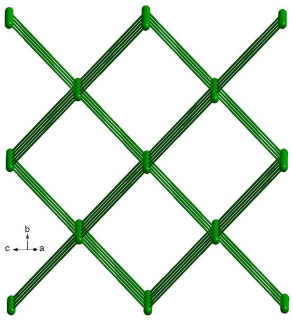

(b)

Fig. 8 (a) View of the 3D network in compound **4** with 1D nanochannel along the *b*-axis. The CdO_4N_2 and PCO_3 polyhedra are shaded in olive and pink, respectively. The ester groups in BPDP ligand toward the channels and guest molecules located at the channels are omitted for clarity. (b) Topological view of the 4-connected $CdSO_4$ net, in which the Cd(II) is simplified as a 4-connected nodes while both ligands are regarded as lines.

Structure differences in all compounds affected by N-donor ligands

The phosphonate monoester ligand in this work only bridges to M(II) cations to form M-BPDP chain because the coordination between M(II) and oxygen from P=O bonds does not occur. The auxiliary N-donor ligands play a crucial role in both structural diversity and dimensionality variation of the resultant MOFs. In compound **1**, BIM ligands act as bridges to connect Cd(II) to chain and the two types of Cd-BPDP and Cd-BIM chains interlock in parallel to afford a 1D double-chain, which are further assembled into a compact three-dimensional structure via van der Waals forces. The BIM connects Cd(II) to give 1D nanoribbons, which are interconnected with Cd-BPDP chains from different directions to construct a 2D thick double-layered structure for compound **2**. The TIB ligand behaving as a 3-connected node connects Co(II) to result in a graphene-like 2D layer, in which two Co(II) cations in the same "6-member ring" are further reinforced by a BPDP bridge, giving rise to a (3,5)-connected layer structure of compound **3**. The TIB ligand in isomorphous compounds **4-6** only bridges to two M(II) to a wave-like chain because one of the three N donors in TIB remains uncoordinated. The cross interconnection of M-BPDP and M-TIB chains leads to a 4-connected 3D network with $CdSO_4$ topology and 1D nanochannels along the *b*-axis.

Moisture Stability

MOFs have shown powerful abilities to tune their composition, structure, pore size/environment as well as structure-related properties in previous reports. However, stability, especially moisture/chemical stability, has being recognized as a very challenging issue for the practical applications of MOFs as functional materials. So far, most of MOFs are more or less sensitive to moisture, which could be one of key limitations to meet the requirements of various applications. The classical Zn_4O-based carboxylate MOFs (such as, MOF-5 or MOF-177 or IRMOF series or UMCM series)[6,22] and many Cd-based carboxylate MOFs[4b,18] are generally moisture- or even air-sensitive, because the bonds between Zn(II)/Cd(II) and carboxylic acid oxygens are not robust enough to tolerate the attack of water molecules. When the carboxylate groups are replaced by phosphonate monoster ligand, $[RPO_2(OCH_2CH_3)]^-$, which may offer two oxygen donor atoms and monoanionic charge, similar to those carboxylates. The additional ethyl groups in the phosphonate monoester might act as a sterically shield to protect M-O bonds and thus improve the moisture stability of resultant MOFs. As expected, the obtained compounds present enhanced stability towards moisture. As shown in Fig. 9, the powder X-ray diffraction (XRD) indicates that the MOFs have very good stability and their frameworks retain well upon exposure to moisture with 30-50% humidity for a couple of days. The results have elegantly demonstrated the superiority regarding misture stability of MOFs based on phosphonate monoester.

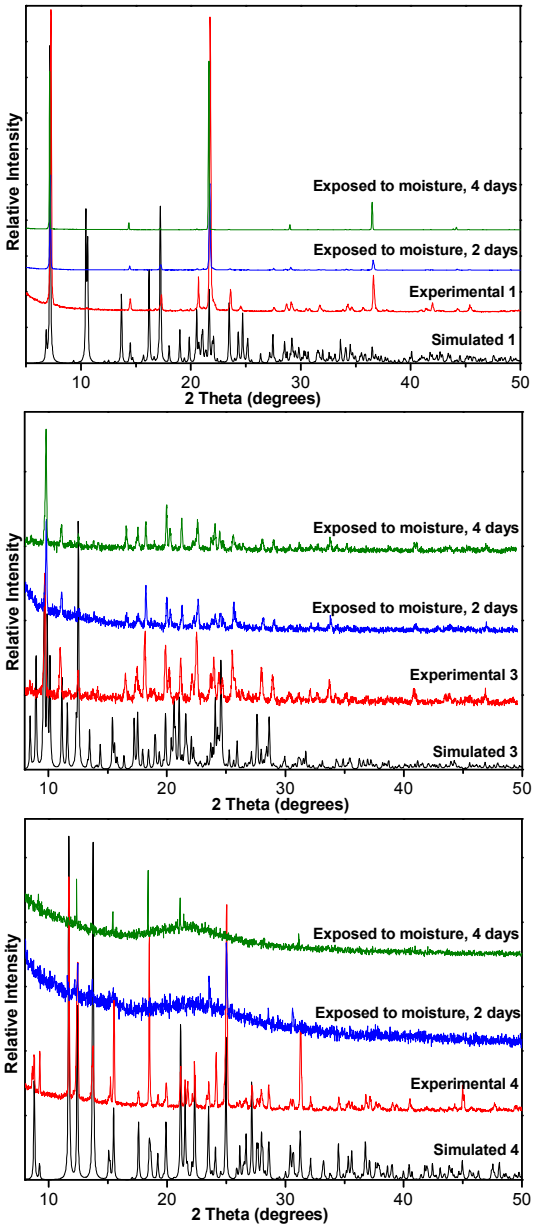

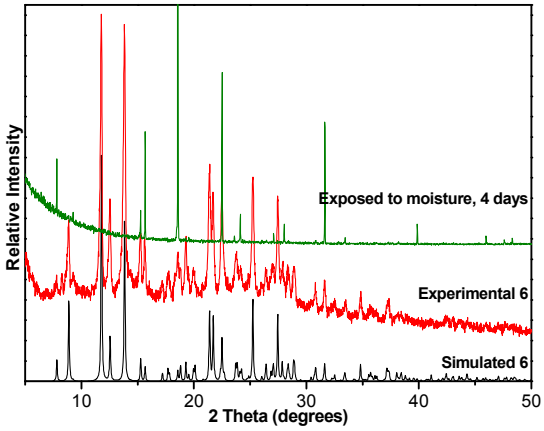

Fig. 9 Powder XRD profiles of simulated and experimental **1**, **3**, **4** and **6**, and their powder XRD patterns upon exposure to moisture (40-50% humidity for **1** and **4**; 30% humidity for **3** and **6**) for 2 and 4 days.

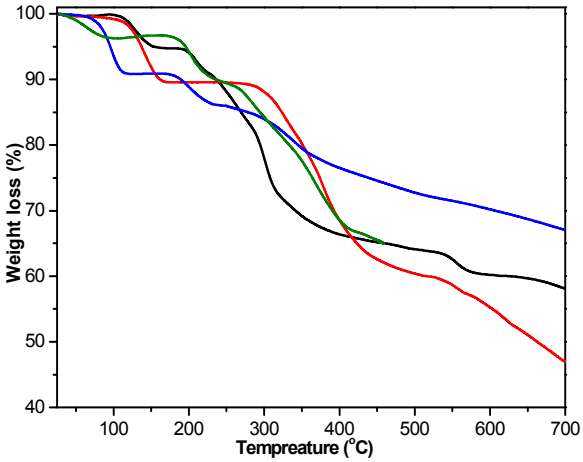

Fig. 10 TG curves for compounds **1** (black), **3** (red), **4** (blue) and **6** (olive).

Thermogravimetric Analysis

Almost all compounds exhibit two main steps of weight loss, for which the first step corresponds to the isolated or/and coordinated water molecule removal and the framework collapses in the second weight loss, as shown in Fig. 10. The decomposition of all compounds does not complete after thermogravimetric (TG) analysis until 700 °C, which has been reported for metal phosphonate compounds.[23] TG curve of compound **1** shows that the first step startes at 100 °C and completed at 165 °C, which corresponds to the release of two coordinated water molecules. The observed weight loss is exactly the same as the calculated value (5.2%). After a short plateau, the combustion of the organic ligands starts from 184 °C. TG curve of compound **3** indicates that it starts to lose weight from room temperature very slowly until ~100 °C, then rapidly loses weight and ends at 168 °C, releasing the isolated and coordinated water molecules. The observed weight loss of 10.5% is lower than the calculated value (16.4%). It should be mentioned such deviation is common for MOFs and usually caused by the spontaneous evaporation of uncoordinated solvents during the sample handling process prior to TG experiment, especially when the compound contains a larger number of lattice solvent molecules. After a long plateau to 275 °C, the organic ligands start to combust and the weight loss does not end until 700 °C. Given the structure similarity, the weight loss curves of compounds **4** and **6** are comparable. Compound **4** slowly loses its weight from room temperature and then rapidly loses weight from 50 to 120 °C, corresponding to the release of isolated solvent molecules. Similarly, the weight loss of compound **6** between room temperature and 100 °C should be caused by the removal of uncoordinated water molecules. In this step, the observed weight losses of 9.1% and 3.7%, respectively for compounds **4** and **6**. Both values are lower than the calculated ones, possibly caused by the spontaneous loss of partial isolated H_2O molecules in air for both compounds before TG experiment. There are a plateau for both compounds **4** and **6** before the second weight loss starting at 170 °C, which should be initiated by coordinated water molecule removal and further triggers the combustion of the organic ligands and framework collapse.

Gas adsorption properties

The gas sorption for MOFs based on phosphonate ligands are seldom studied because the common phosphonic acid offers three coordinated oxygens to metal cations and the resultant metal phosphonates are usually nonporous or of tiny pore. Phosphonate monoester as carboxylate linker gave MOFs with suitable pore sizes and certain gas sorption capabilities in previous reports.[12c-e] In this work, it behaves as a bridge to connect metal ions to porous 3D frameworks of compounds **4-6** with moderate 1D nanochannels. Upon removal solvent molecules by evacuation, the CO_2 adsorption studies at 195 K for compounds **4** and **6** have shown around 30 cm^3/g and 40 cm^3/g, respectively. The results reveals the presence of permanent porosity and corresponds to the Langmuir surface areas of 16 and 70 m^2/g, respectively for compounds **4** and **6.**

Fluoresence Properties

The solid-state luminescence properties of compounds **1**, **4**, **6** as well as the BPDP, BIM and TIB ligands were investigated at room temperature (Fig. 11 and S10). The BPDP and BIM ligands exhibit fluorescence emission bands at λ_{max} = 340 and 347 nm, respectively under excitation at 278 nm. Upon combination of both BPDP and BIM ligands with the Cd(II) ions, compound **1** displays a strong fluorescence emission band at λ_{max} = 346 nm (λ_{ex} = 278 nm), which is very close to that of ligand emission and thus could be originated from the intraligand transitions. The TIB ligand displays weak and broad fluorescence emission ranging from 378 to 392 nm upon excitation at 330 nm. Under the same exitation, compound **4** emits strong solid-state fluorescence at λ_{max} = 387 nm, which might also be assigned to intraligand transitions. The very weak fluorescence intensity of compound **6** could be due to the qenching effect of Cu(II) ions.

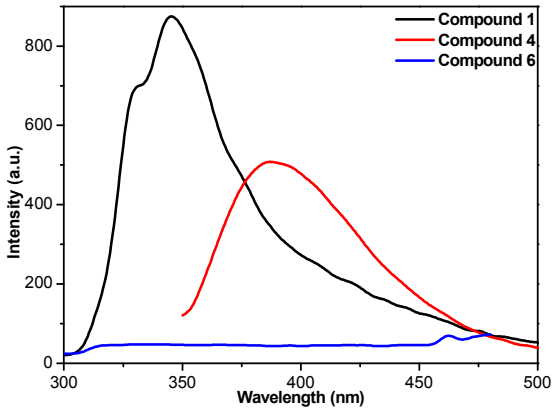

Fig. 11 Solid-state emission spectra of compounds **1** (black, λ_{ex} = 278 nm), **4** (red, λ_{ex} = 330 nm), and **6** (blue, λ_{ex} = 253 nm) at room temperature.

Conclusions

In conclusion, six MOFs with structure dimensionality from 1D to 3D have been synthesized based on a phosphonate monoester ligand. The auxiliary N-donor ligands, BIM and TIB, have shown subtle effects for the structural diversity and dimensionality variation of the resultant MOFs. More importantly, with the steric protection of ethyl groups (in BPDP ligand) as a shield for the hydrolytically vulnerable M-O bonds, the obtained MOFs have considerable stability and remain stable upon exposure to moisture with 30-50% humidity for 2-4 days, which would facilitate their functional applications. The MOFs with 3D porous network have presented CO_2 gas sorption properties and revealed their permanent porosity. The Cd-based MOFs have also shown strong fluorescence emissions assigned to intraligand transitions. The successful preparation of these MOFs based on an elongated phosphonate bis(monoester) ligand provides a valuable approach for the construction of MOFs with tuneable structures and improved moisture stability. The exploration of phosphonate monoester moiety in other ligand skeletons for MOF synthesis is currently underway in our laboratory.

Acknowledgements

This work was supported by the National Natural Science Foundation of China (21361002, Z.Y.D.; 21371162 and 51301159, H.L.J.), and the Young Scientists Training Program of Jiangxi Province (20122BCB23020, Z.Y.D.). H.L.J. also thanks Research Fund for the Doctoral Program of Higher Education of China (20133402120020), Scientific Research Foundation for the Returned Overseas Chinese Scholars, State Education Ministry and the Fundamental Research Funds for the Central Universities (WK2060190026).

Notes and references

[a]College of Chemistry and Chemical Engineering, Gannan Normal University, Ganzhou 341000, P.R. China
E-mail: ziyidu@gmail.com (Z.Y.D.)
[b]Hefei National Laboratory for Physical Sciences at the Microscale, Department of Chemistry, University of Science and Technology of China, Hefei, Anhui 230026, P.R. China
E-mail: jianglab@ustc.edu.cn (H.L.J.) Fax: +86-551-63607861
[c]State Key Laboratory of Structural Chemistry, Fujian Institute of Research on the Structure of Matter, Chinese Academy of Sciences, Fuzhou, Fujian 350002, P.R. China

†Electronic Supplementary Information (ESI) available: X-ray crystallographic files (CCDC Nos. 978185-978192) for ligands and compounds **1-6** in CIF format, organic ligand synthesis and additional figures. For ESI and crystallographic data in CIF or other electronic format See DOI: 10.1039/b000000x/

1 (a) S. Horike, S. Shimomura and S. Kitagawa, *Nat. Chem.*, 2009, **1**, 695; (b) J. R. Long and O. M. Yaghi, *Chem. Soc. Rev.*, 2009, **38**, 1213; (c) Z. Wang and S. M. Cohen, *Chem. Soc. Rev.*, 2009, **38**, 1315; (d) J. J. Perry IV, J. A. Perman and M. J. Zaworotko, *Chem. Soc. Rev.*, 2009, **38**, 1400; (e) H.-C. Zhou, J. R. Long and O. M. Yaghi, *Chem. Rev.*, 2012, **112**, 673.

2 (a) H. Wu, W. Zhou and T. Yildirim, *J. Am. Chem. Soc.*, 2009, **131**, 4995; (b) R. Vaidhyanathan, S. S. Iremonger, G. K. H. Shimizu, P. G. Boyd, S. Alavi and T. K. Woo, *Science*, 2010, **330**, 650; (c) K. Sumida, D. L. Rogow, J. A. Mason, T. M. McDonald, E. D. Bloch, Z. R. Herm, T.-H. Bae and J. R. Long, *Chem. Rev.*, 2012, **112**, 724; (d) M. P. Suh, H. J. Park, T. K. Prasad and D.-W. Lim, *Chem. Rev.*, 2012, **112**, 782; (e) J.-R. Li, J. Sculley and H.-C. Zhou, *Chem. Rev.*, 2012, **112**, 869.

3 (a) J. S. Seo, D. Whang, H. Lee, S. I. Jun, J. Oh, Y. J. Jeon and K. Kim, *Nature*, 2000, **404**, 982; (b) L. Ma, C. Abney and W. Lin, *Chem. Soc. Rev.*, 2009, **38**, 1248; (c) D. Farrusseng, S. Aguado and C. Pinel, *Angew. Chem. Int. Ed.*, 2009, **48**, 7502; (d) A. Corma, H. García and F. X. Llabrés i Xamena, *Chem. Rev.*, 2010, **110**, 4606; (e) H.-L. Jiang and Q. Xu, *Chem. Commun.*, 2011, **47**, 3351; (f) Z. Zhang, L. Zhang, L. Wojtas, M. Eddaoudi and M. J. Zaworotko, *J. Am. Chem. Soc.*, 2012, **134**, 928.

4 (a) B. Chen, S. Xiang and G. Qian, *Acc. Chem. Res.*, 2010, **43**, 1115; (b) H.-L. Jiang, Y. Tatsu, Z.-H. Lu and Q. Xu, *J. Am. Chem. Soc.*, 2010, **132**, 5586; (c) Y. Takashima, V. Martinez, S. Furukawa, M. Kondo, S. Shimomura, H. Uehara, M. Nakahama, K. Sugimoto And S. Kitagawa, *Nat. Commun.*, 2011, **2**, 168; (d) L. E. Kreno, K. Leong, O. K. Farha, M. Allendorf, R. P. Van Duyne and J. T. Hupp, *Chem. Rev.*, 2012, **112**, 1105.

5 (a) J. An, S. J. Geib and N. L. Rosi, *J. Am. Chem. Soc.*, 2009, **131**, 8376; (b) J. D. Rocca, D. Liu and W. Lin, *Acc. Chem. Res.*, 2011, **44**, 957; (c) P. Horcajada, R. Gref, T. Baati, P. K. Allan, G. Maurin, P. Couvreur, G. Férey, R. E. Morris and C. Serre, *Chem. Rev.*, 2012, **112**, 1232.

6 (a) H. Li, M. Eddaoudi, M. O'Keeffe and O. M. Yaghi, *Nature*, 1999, **402**, 276; (b) J. A. Greathouse and M. D. Allendorf, *J. Am. Chem. Soc.*, 2006, **128**, 10678; (c) S. S. Kaye, A. Dailly, O. M. Yaghi, and J. R. Long, *J. Am. Chem. Soc.*, 2007, **129**, 14176.

7 (a) K. S. Park, Z. Ni, A. P. Côté, J. Y. Choi, R. Huang, F. J. Uribe-Romo, H. K. Chae, M. O'Keeffe and O. M. Yaghi, *Proc. Natl. Acad. Sci. U.S.A.*, 2006, **103**, 10186; (b) X. C. Huang, Y. Y. Lin, J. P. Zhang and X. M. Chen, *Angew. Chem., Int. Ed.*, 2006, **45**, 1557; (c) G. Férey, C. Mellot-Draznieks, C. Serre, F. Millange, J. Dutour, S. Surblé and I. Margiolaki, *Science*, 2005, **309**, 2040; (d) G. Férey, C. Serre, C. Mellot-Draznieks, F. Millange, S. Surblé, J. Dutour and I. Margiolaki, *Angew. Chem. Int. Ed.*, 2004, **43**, 6296.

8 (a) J. H. Cavka, S. Jakobsen, U. Olsbye, N. Guillou, C. Lamberti, S. Bordiga and K. P. Lillerud, *J. Am. Chem. Soc.*, 2008, **130**, 13850; (b) V. Colombo, S. Galli, H. J. Choi, G. D. Han, A. Maspero, G. Palmisano, N. Masciocchi and J. R. Long, *Chem. Sci.*, 2011, **2**, 1311.

9 (a) H.-L. Jiang, D. Feng, T.-F. Liu, J.-R. Li and H.-C. Zhou, *J. Am. Chem. Soc.*, 2012, **134**, 14690; (b) D. Feng, Z.-Y. Gu, J.-R. Li, H.-L. Jiang, Z. Wei and H.-C. Zhou, *Angew. Chem. Int. Ed.*, 2012, **51**, 10307; (c) H.-L. Jiang, D. Feng, K. Wang, Z.-Y. Gu, Z. Wei, Y.-P. Chen and H.-C. Zhou, *J. Am. Chem. Soc.*, 2013, **135**, 13934; (d) D. Feng, W.-C. Chung, Z. Wei, Z.-Y. Gu, H.-L. Jiang, D. J. Darensbourg and H.-C. Zhou, *J. Am. Chem. Soc.*, **2013**, **135**, 17105; (e) D. Feng, H.-L. Jiang, Y.-P. Chen, Z.-Y. Gu, Z. Wei and H.-C. Zhou, *Inorg. Chem.*, 2013, **52**, 12661.

10 (a) J. H. Cavka, S. Jakobsen, U. Olsbye, N.Guillou, C. Lamberti, S. Bordiga and K. P. Lillerud, *J. Am. Chem. Soc.*, 2008, **130**, 13850; (b) M. Kandiah, M. H. Nilsen, S. Usseglio, S. Jakobsen, U. Olsbye, M. Tilset, C. Larabi, E. A. Quadrelli, F. Bonino and K. P. Lillerud, *Chem. Mater.*, 2010, **22**, 6632; (c) A. Schaate, P. Roy, A. Godt, J. Lippke, F. Waltz, M. Wiebcke and P. Behrens, *Chem. Eur. J.*, 2011, **17**, 6643; (d) A. Schaate, P. Roy, T. Preuße, S. J. Lohmeier, A. Godt and P. Behrens, *Chem. Eur. J.*, 2011, **17**, 9320; (e) W. Morris, B. Volosskiy, S. Demir, F. Gándara, P. L. McGrier, H. Furukawa, D. Cascio, J. F. Stoddart and O. M. Yaghi, *Inorg. Chem.*, 2012, **51**, 6443; (f) V. Bon, V. Senkovskyy, I. Senkovska and S. Kaskel, *Chem. Commun.*, 2012, **48**, 8407; (g) V. Guillerm, F. Ragon, M. Dan-Hardi, T. Devic, M. Vishnuvarthan, B. Campo, A. Vimont, G. Clet, Q. Yang, G. Maurin, G. Férey, A. Vittadini, S. Gross and C. Serre, *Angew. Chem. Int. Ed.*, 2012, **51**, 9267.

11 (a) A. Clearfield, Metal phosphonate chemistry, in *Progress in Inorganic Chemistry*, ed. K. D. Karlin, 1998, **47**, 371, Wiley, New York; (b) K. Maeda, *Microporous Mesoporous Mater.*, 2004, **73**, 47; (c) J.-G. Mao, *Coord. Chem. Rev.*, 2007, **251**, 1493; (d) G. K. H. Shimizu, R. Vaidhyanathan, J. M. Taylor, *Chem. Soc. Rev.*, 2009, **38**, 1430; (e) K. J. Gagnon, H. P. Perry, A. Clearfield, *Chem. Rev.*, 2012, **112**, 1034.

12 (a) O. R. Evans, D. R. Manke and W. Lin, *Chem. Mater.*, 2002, **14**, 3866; (b) M. Kontturi, E. Laurila, R. Mattsson, S. Pera□niemi, J. J. Vepsa□la□inen and M. Ahlgrén, *Inorg. Chem.*, 2005, **44**, 2400; (c) S. S. Iremonger, J. Liang, R. Vaidhyanathan and G. K. H. Shimizu, *Chem. Commun.*, 2011, **47**, 4430; (d) S. S. Iremonger, J. Liang, R. Vaidyanathan, I. Martens, G. K. H. Shimizu, T. D. Daff, M. Z. Aghaji, S. Yeganegi and T. K. Woo, *J. Am. Chem. Soc.*, 2011, **133**, 20048; (e) J. M. Taylor, R. Vaidhyanathan, S. S. Iremonger and G. K. H. Shimizu, *J. Am. Chem. Soc.*, 2012, **134**, 14338; (f) T. Yamada and H. Kitagawa, *CrystEngComm*, 2012, **14**, 4148.

13 J. G. Nguyen and S. M. Cohen, *J. Am. Chem. Soc.*, 2010, **132**, 4560.

14 (a) C. R. Mayer, M. Hervé, H. Lavanant, J.-C. Blais and F. Sécheresse, *Eur. J. Inorg. Chem.*, 2004, 973; (b) J. Cai, T. Zhao, G. An, B. Zhou and Q. Hu, *Chem. Bioeng. (in Chinese)*, 2009, **26**, 22; (c) A. Rit, T. Pape, A. Hepp and F. E. Hahn, *Organometallics*, 2011, **30**, 334.

15 *APEX2, SADABS and SAINT.* Bruker AXS Inc.: Madison, Wisconsin, USA. 2008.

16 (a) G. M. Sheldrick, SHELXS-97, *Program for X-ray Crystal Structure Solution*, University of Göttingen, Germany, 1997; (b) G. M. Sheldrick, SHELXL-97, *Program for X-ray Crystal Structure Refinement*, University of Göttingen, Germany, 1997.

17 A. L. Spek, *Acta Crystallogr. Sect. D*, 2009, **65**, 148.

18 (a) H. Yang, F. Wang, Y.-X. Tan, T.-H. Li and J. Zhang, *Chem. Asian J.*, 2012, **7**, 1069; (b) J. Guo, D. Sun, L. Zhang, Q. Yang, X. Zhao and D. Sun, *Cryst. Growth Des.*, 2012, **12**, 5649.

19 (a) L. Chen, G.-J. Xu, K.-Z. Shao, Y.-H. Zhao, G.-S. Yang, Y.-Q. Lan, X.-L. Wang, H.-B. Xu and Z.-M. Su, *CrystEngComm*, 2010, **12**, 2157; (b) W. Yang, M. Guo, F.-Y. Yi and Z.-M. Sun, *Cryst. Growth Des.*, 2012, **12**, 5529; (c) T. Panda, K. M. Gupta, J. Jiang and R. Banerjee, *CrystEngComm* , 2014, DOI: 10.1039/c3ce42075b.

20 A. L. Spek, *J. Appl. Crystallogr.*, 2003, **36**, 7.

21 (a) A. F. Wells, *Three-Dimensional Nets and Polyhedra*, Wiley: New York, **1977**; (b) S. R. Batten and R. Robson, *Angew. Chem. Int. Ed.*, 1998, **37**, 1460; (c) N. W.Ockwig, O. Delgado-Fridedrichs, M. O'Keeffe and O. M. Yaghi, *Acc. Chem. Res.*, 2005, **38**, 176.

22 (a) M. Eddaoudi, J. Kim, N. Rosi, D. Vodak, J. Wachter, M. O'Keeffe and O. M. Yaghi, *Science*, 2002, **295**, 469; (b) H. K. Chae, D. Y. Siberio-Pérez, J. Kim, Y. Go, M. Eddaoudi, A. J. Matzger, M. O'Keeffe and O. M. Yaghi, *Nature*, 2004, **427**, 523; (c) K. Koh, A. G. Wong-Foy and A. J. Matzger, *Angew. Chem. Int. Ed.*, 2008, **47**, 677; (d) K. Koh, A. G. Wong-Foy and A. J. Matzger, *J. Am. Chem. Soc.*, 2009, **131**, 4184.

23 Z.-Y. Du, X.-L. Li, Q.-Y. Liu and J.-G. Mao, *Cryst. Growth Des.*, 2007, **7**, 1501.

Graphical Abstract

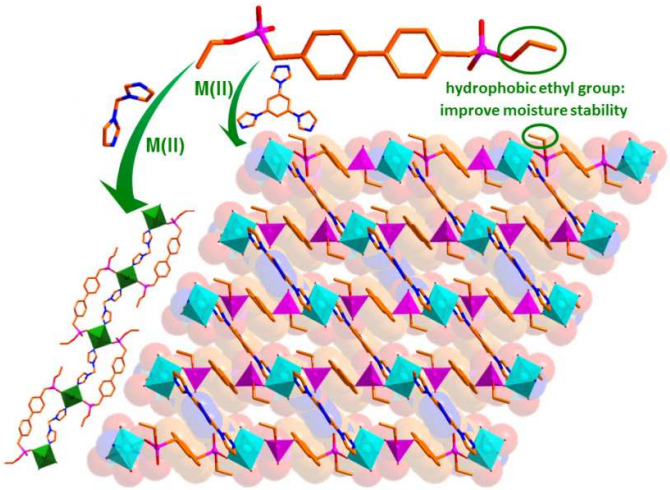

A series of metal-organic frameworks (MOFs) with improved moisture stability, featuring 1D chain, 2D layer and 3D network, have been obtained based on phosphonate monoester in the presence of auxiliary N-donor ligands.